Polymer 50 (2009) 3600–3608

Contents lists available at ScienceDirect

Polymer

journal homepage: www.elsevier.com/locate/polymer

Dispersions of carbon nanotubes in sulfonated poly[bis(benzimidazobenziso-quinolinones)] and their proton-conducting composite membranes

Nanwen Li [a,b], Feng Zhang [a,b], Junhua Wang [a,b], Shenghai Li [a], Suobo Zhang [a,*]

[a] State Key Laboratory of Polymer Physics and Chemistry, Changchun Institute of Applied Chemistry, Chinese Academy of Sciences, Changchun 130022, Jilin, China
[b] Graduate School of Chinese Academy of Sciences, China

ARTICLE INFO

Article history:
Received 26 February 2009
Received in revised form
7 May 2009
Accepted 14 May 2009
Available online 22 May 2009

Keywords:
Sulfonated poly[bis(benzimidazo-benzisoquinolinones)]
Carbon nanotubes
Proton exchange membranes

ABSTRACT

A sulfonated poly[bis(benzimidazobenzisoquinolinones)] (SPBIBI) possessing a conjugated pyridinone ring was shown to be effective for dispersing multiwalled carbon nanotubes (MWCNTs) in DMSO. The dispersions in which the SPBIBI to MWCNTs mass ratio was 4:1 demonstrated the highest MWCNTs concentrations, i.e., 1.5–2.0 mg mL^{-1}, and were found to be stable for more than six months at room temperature. Through casting of these dispersions, MWCNTs/SPBIBI composite membranes were successfully fabricated on substrates as proton exchange membranes for fuel cell applications and showed no signs of macroscopic aggregation. The properties of composite membranes were investigated, and it was found that the homogeneous dispersion of the MWCNTs in the SPBIBI matrix altered the morphology structures of the composite membranes, which lead to the formation of more regular and smaller cluster-like ion domains. As a result, and in comparison to a pristine SPBIBI membrane, the composite membranes displayed more significant proton conductivities, especially at low relative humidity, without sacrificing other excellent properties, such as thermal, dimensional and oxidative stabilities. For instance, the composite membranes with an MWCNTs content only of 0.5 wt% exhibited proton conductivities of 0.021 S cm^{-1} at 50 RH% and 70 °C, a value almost fourfold as high as that of the pristine SPBIBI membranes under identical conditions (0.005 S cm^{-1}). The result was comparable to Nafion 117 (0.021 S cm^{-1}). The homogenous dispersion of the MWCNTs and the efficient enhancement the SPBIBI performance were attributed to the π–π interaction between the pyridinone ring and the sidewalls of the MWCNTs which changed the morphological structure of composite membranes as revealed by TEM. A combination of a low methanol crossover with excellent thermo-oxidative and water stabilities indicated that the SPBIBI composite membranes were good candidate materials for proton exchange membranes in fuel cell applications.

1. Introduction

Polymer electrolyte membranes constitute an important class of polymeric materials for use as ion exchangers, electrolytes for batteries and sensors, and dopants for electronic conductors. In particular, recent progress in the area of polymer electrolyte membrane fuel cells (PEMFCs) has stimulated considerable interest in proton-conductive electrolyte membranes (PEMs) [1,2]. For a fuel cell to work effectively and to be widely adapted, the PEM must have a portfolio of properties including an acceptable costs, a high proton conductivity, good chemical and thermal stabilities, a good mechanical strength, and a low fuel crossover [3]. A current state-of-the-art PEMs material is Nafion; a perfluorinated ionomer developed by DuPont. Nafion has demonstrated a superior chemical and electrochemical stabilities, in addition to a high proton conductivity with a relatively low ion exchange capacity (IEC) [4,5]. However, the material has several shortcomings that limit its utility and performance, such as a low proton conductivity at elevated temperatures, a high methanol diffusion, and significant manufacturing costs [6–10]. Resultantly, much progress has been made to develop novel proton exchange membranes based on sulfonated aromatic polymers due to their good physical properties and the fact that they are inexpensive [3,11–24]. Traditionally, aromatic ionomer membranes reach suitable proton conductivities only at high degrees of sulfonation due to a lack of ion channel and the lower acidity of aryl-sulfonic acid as compared to Nafion [3,7]. However, a high degree of sulfonation leads to a significant degradation of the physical properties (oxidative, hydrolytic and dimensional stabilities) of humidified polymers and also causes an increase in methanol diffusion.

* Corresponding author. Tel.: +86 4315605139.
E-mail address: sbzhang@ciac.jl.cn (S. Zhang).

0032-3861/$ – see front matter © 2009 Elsevier Ltd. All rights reserved.
doi:10.1016/j.polymer.2009.05.028

Few membranes have displayed the combination of high proton conductivities and stabilities (especially at elevated temperatures) with a low methanol crossover. The stability and proton conductivity of aromatic PEMs remain issues, and must thus be improved [25,26]. For these reasons, researchers have synthesized and investigated modified membranes, prepared by using hygroscopic inorganic fillers such as SiO_2 [27], nanoclay [28], inorganic particles [29], or a polymer hybrid [30–33]. Despite that such composite membranes have shown enhanced mechanical properties or lower methanol permeabilities, the effect of the composite on the proton conductivity is not very distinct or even negative in some cases. In addition to the chemical and physical state of the inorganic "fillers", the procedure for fabricating the membranes also seems crucial, as absorbed water can take part in proton conduction only when located in the vicinity of acid groups of the matrix polymers.

Currently, carbon nanotubes (CNTs) attract much attention as a new class of advanced "filler" materials because of their interesting properties and the possibility of employing them in emerging applications in nanoelectronics as well as in the field of nanocomposites [34–36]. The CNTs/Nafion composites have been used in for instance actuators, microscopic pumps, sensors, and electrocatalysts [37,38]. Furthermore, Liu et al. have reported on using them as electrolyte, however without obtaining any significant improvement in performance despite the higher mechanical stability [39]. Functionalized composites of CNTs with Nafion have displayed a reduced methanol crossover, but suffer from poor proton conductivities [40]. Moreover, the strong intrinsic van der Waals forces of CNTs as well as the lack of interfacial interactions between CNTs and Nafion limit the dispersion of CNTs at higher loadings in addition to the load transfer from the Nafion matrix to the nanotubes. The potential advantages of using CNTs to improve the portfolio performance in PEM fuel cells have therefore not been fully realized, and it is important to enhance the interfacial interactions between the CNTs and polymers in order to obtain a homogeneous dispersion and thus also an enhancement of the properties of the composite membranes [41,42]. Aromatic condensation polymers such as polyimide [43–45] and polybenzimidazole [46] with conjugated groups have been reported to be excellent for dispersing CNTs and enhancing the mechanical strength or electrical conductivities of composites for use in the aerospace industry. This is due to the strong interfacial interactions (such as π–π interactions) between the conjugated groups of the polymers and the sidewalls of the CNTs. To the best of our knowledge, the homogenous dispersion of CNTs into aromatic ionomers matrixes for proton exchange membranes and the study of the effect of the dispersed CNTs on the properties, especially the proton conductivity of the composites, have not yet been carried out. It should hence be interesting to monitor the proton conductivity of aromatic ionomers into which homogeneous dispersions of CNTs have been introduced.

The objective of the present research was to elucidate the effect on material properties of multiwalled carbon nanotubes (MWCNTs) incorporated into aromatic ionomers and thus to produce highly proton-conductive composite membranes. A sulfonated poly [bis(benzimidazobenzisoquinolinones)] (SPBIBI) with a conjugated pyridinone ring was chosen as the matrix polymer due to its excellent thermo-oxidative, hydrolytic and dimensional stabilities as a proton exchange membrane [47,48]. The conjugated pyridinone ring of the SPBIBI, as shown in Fig. 1, was able to form strong interactions (such as π–π interactions) with the sidewalls of the MWCNTs, while the sulfonic acid groups provided the debundled MWCNTs with a good solubility and stability in organic solvents and host polymer matrices. From the homogenous dispersions, novel polymer nanocomposite membranes composed of SPBIBI and MWCNTs could be fabricated for use in proton exchange applications without any sign of macroscopic aggregation. These hydrophobic MWCNTs interacted with pyridinone ring and located in the hydrophobic domains of polymer matrix, they were except to exquisitely tune the extent of networking in the matrix and thus increase the hydrophilic/hydrophobic separation of the composite membranes. The increased hydrophilic/hydrophobic separation would naturally help to increase the proton conductivities without sacrificing other excellent properties (such as thermo-oxidative or dimensional stabilities) in the composite membranes. Moreover, the high affinity of the SPBIBI for the MWCNTs allowed the polymers to completely coat and insulate the surfaces of the MWCNTs, thereby lowering the risk for short-circuiting.

2. Experimental

2.1. Materials

SPBIBI and SPBIBI-b were synthesized according the method previously reported [47,48]. The multiwalled carbon nanotubes (MWCNTs) used in this work were purchased from Chendu organic chemicals Co. Ltd., China (purity > 95%, length 1–2 μm, diameter 10–20 nm). All other regent were obtained from commercial sources and used as received.

2.2. Preparation and characterization of MWCNTs/SPBIBI dispersion

MWCNTs/SPBIBI was dispersed in DMSO by mixing with SPBIBI followed by sonication for 1 h with the water bath temperature maintained at 50 °C. The dispersed MWCNTs were analyzed by TEM on JEM-1011 operating at 100 kV and UV–vis–near IR spectra

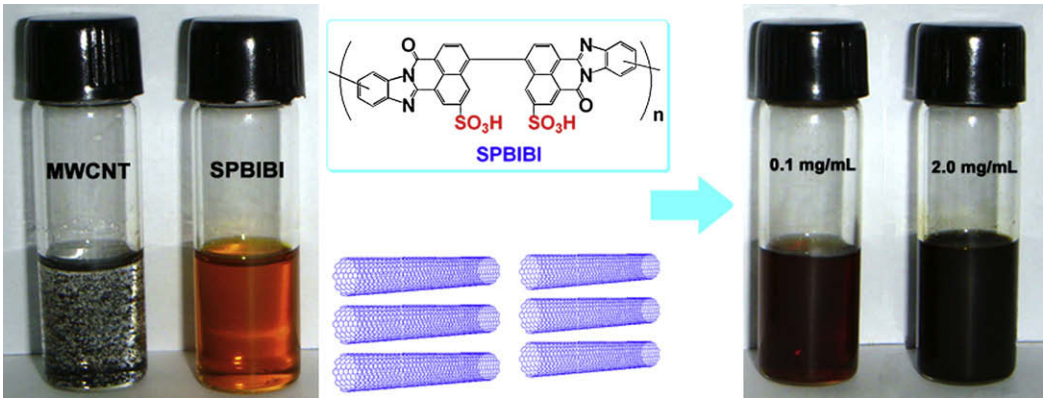

Fig. 1. The procedure for the formation of homogenous MWCNT/SPBIBI dispersions in DMSO.

(JASCO). Fluorescence measurements were conducted on a Fluorolog-3 spectrofluorometer system and the UV–vis spectra were measured with a Shimadze Uv-2550 spectrometer in the transmittance mode. ^{1}H NMR spectra were measured at 600 MHz on Bruker AV 600 spectrometer.

2.3. Preparation of MWCNTs/SPBIBI composite membranes

The MWCNTs (5 mg) were added to the SPBIBI (500 mg) in DMSO (10 mL) and then the mixture was sonicated for 30 min using a probe-type sonicator (Ultrasonic Disreptor UD-200, TOMY; 46W), followed by centrifugation at 3700 rpm for 30 min. The DMSO dispersion of the MWCNTs/SPBIBI composite was cast onto glass substrates, followed by drying at 100 °C for 12 h. The as-cast composite membranes were dried in vacuum at 150 °C for 12 h to remove the residual solvent.

2.4. Measurements

FT-IR spectra were obtained with a Bio-Rad digilab Division FTS-80 FT-IR spectrometer. The thermogravimetric analyses (TGA) were obtained in nitrogen with a Perkin-Elemer TGA-2 thermogravimetric analyzer at a heating rate of 10 °C min^{-1}.

The ion exchange capacity (IEC) was measured by classical titration. The membranes in the H^+ form were immersed in a 1 M NaCl solution for 24 h to liberate the H^+ ions (the H^+ ions in the membrane were replaced by Na^+ ions). The H^+ ions in solution were then titrated with 0.01 M NaOH using phenolphthalein as an indicator.

2.5. Water uptake and swelling ratio

The membrane (30–40 mg per sheet) was dried at 100 °C under vacuum for 6 h until constant weight as dry material was obtained. It was immersed into deionized water at room temperature for 4 h. Then the membranes were taken out, wiped with tissue paper, and quickly weighted on a microbalance. Water uptake of the membranes was calculated from:

$$\text{Water uptake (wt\%)} = \text{WU} = \left(W_{\text{wet}} - W_{\text{dry}}\right)\Big/W_{\text{dry}} \quad (1)$$

Water swelling ratio of the membranes were investigated by immersing the round shape samples into water at room temperature for a given time, the changes of through-plan and in-plane direction were calculated as following:

$$\Delta\text{Tc} = (T - Ts)/Ts$$

$$\Delta\text{Lc} = (L - Ls)/Ls \quad (2)$$

where *Ts* and *Ls* are the through-plan and in-plane direction of the membrane at dry state, respectively; *T* and *L* refer to those of the membrane immersed in liquid water for 5 h.

2.6. Electron, proton conductivity and methanol permeability measurement

Electrical conductivity of the dried membranes was measured at room temperature by standard four-probe method using a Keithley 2400 instrument. The resistivity indicator operated at 9 V and reported as an average of three readings. The electron conductivity was calculated by the following equation: $\sigma = dI/(L_sW_sU)$ (d: distance between reference electrodes, and L_s and W_s are the thickness and width of the dried membrane, respectively). All membranes were dried at 150 °C in vacuum for 10 h before measurement.

The proton conductivity (σ, S cm^{-1}) of each membrane coupon (size: 1 cm × 4 cm) was obtained using $\sigma = d/L_sW_sR$ (d: distance between reference electrodes, and L_s and W_s are the thickness and width of the membrane, respectively). The resistance value (R) was measured over the frequency range from 100 mHz to 100 kHz by four-point probe alternating current (ac) impedance spectroscopy using an electrode system connected with an impedance/gain-phase analyzer (Solatron 1260) and an electrochemical interface (Solatron 1287, Farnborough Hampshire, ONR, UK). The membranes were sandwiched between two pairs of gold-plate electrodes. Conductivity measurements under fully hydrated conditions were carried out with the cell immersed in liquid water. For the measurement above 100 °C at 100% RH, a pressure-resistant closed chamber was used. At a given temperature, the samples were equilibrated for at least 30 min before any measurements. The proton conductivities at 70 °C, 50% RH were also studied. Typically, the membranes were placed in a humidity chamber (the relative humidity was controlled at 50% by saturated NaBr aqueous at 70 °C) for at least 24 h before measurements.

The methanol permeability was determined by using a cell basically consisting of two-half-cells separated by the membrane, which was fixed between two rubber rings. Methanol (2 mol L^{-1}) was placed on one side of the diffusion cell, and water was placed on the other side. Magnetic stirrers were used on each compartment to ensure uniformity. The concentration of the methanol was measured by using a SHIMADZU GC-1020A series gas chromatograph. Peak areas were converted into methanol concentration with a calibration curve. The methanol permeability was calculated by the following equation:

$$C_B(t) = \frac{A}{V_B}\cdot\frac{DK}{L}\cdot C_A\cdot(t - t_0) \quad (3)$$

Where C_A and C_B are the methanol concentration of feed side and permeated through the membrane, respectively. A, L and V_B are the effective area, the thickness of membrane and the volume of permeated compartment, respectively. DK is defined as the methanol permeability. t_0 is the time lag.

3. Results and discussion

3.1. Dispersion of MWCNTs in sulfonated poly[bis(benzimidazobenzisoquinolinone)] (SPBIBI)

MWCNTs were purified with a HCl solution treatment in order to remove residues of metal catalyst. Fig. 1 depicts the formation of the MWCNTs suspensions. Bundled nanotubes were subjected to a 30-min sonication in a SPBIBI/DMSO solution, and following centrifugation of the dispersion, supernatants were collected. The supernatant solution from dispersion is dark, as also illustrated in Fig. 1. The highest possible MWCNTs concentration that could be dispersed in DMSO using SPBIBI was in the range of 1.5–2.0 mg mL^{-1}, and this was higher than the corresponding value (i.e., 0.7–1.2 mg mL^{-1}) obtained with poly(3-hexylthiophene) (P3HT) in chloroform [49]. The as-dispersed MWCNTs were very stable, and did not precipitate even after six months of storage at room temperature. Furthermore, the higher molecular weight (reduced viscosity) of SPBIBI allowed for an enhanced polymer binding due to the incremental additive nature of the attractive interactions, which was similar to P3HT [50]. These results suggest that SPBIBI had an excellent dispersing capability for MWCNTs.

The stability of the MWCNTs/SPBIBI dispersions was further examined through a centrifugation test [49]. After being subjected to a centrifugation test at 10,000 rpm for 30 min, all MWCNTs were found to remain in solution, and such an observation suggested that the SPBIBI was attached to the MWCNT walls through a strong and

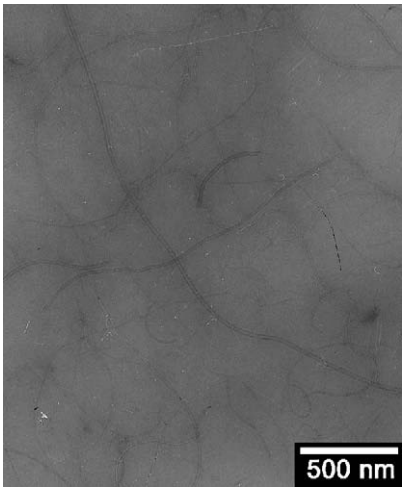

Fig. 2. A TEM micrograph of MWCNTs/SPBIBI with a mass ratio of 1:4.

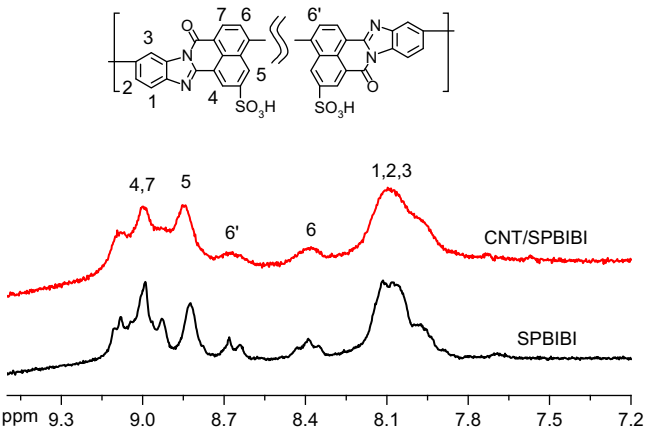

Fig. 4. ^{1}H NMR spectra of MWCNTs/SPBIBI (mass ratio: 1:4) and pristine SPBIBI in DMSO-d_6.

stable molecular interaction, most likely a stacking interaction between the polymers and the carbon nanotubes. The extent of dispersion of the MWCNTs was examined by transmission electron microscopy (TEM). Fig. 2 displays a micrograph of the dispersion and one can see that the majority of the MWCNTs were de-bundled individual tubes with a widths of ~20 nm. Also UV–vis–near IR spectroscopy of the MWCNTs/SPBIBI dispersion was carried out and the obtained spectra are presented in Fig. 3. The characteristic absorption bands of the MWCNTs were clearly visible in the 600–1600 nm region, implying an effective dispersion of the MWCNTs in the mixture [51]. Furthermore, the absorbance of the MWCNTs remained unchanged—even after a time period of six months—thus confirming the stability of the MWCNTs/SPBIBI dispersion.

The MWCNTs/SPBIBI dispersion was further investigated by ^{1}H NMR and optical spectroscopy. Fig. 4 shows ^{1}H NMR spectra of pristine SPBIBI and of the MWCNTs/SPBIBI (mass ratio 1:4) dispersion along with the proton assignment. A broadening of the proton peaks was observed, and when compared to those from the pristine SPBIBI, their intensity was found to be reduced. Previous studies have revealed that the interactions of polymers with MWCNTs have caused broadening and a reduced intensity of ^{1}H NMR peaks [52,53]. Accordingly, the present results from the ^{1}H NMR spectral analysis strongly supported the existence of an interaction between the MWCNTs and the SPBIBI. Fig. 5 presents the UV–vis absorption spectra that were obtained from a dilute solution (0.06 mg mL^{-1}) of the polymer and the MWCNTs/SPBIBI dispersion in DMSO. Three major absorption bands were observed for SPBIBI, with values 269, 312 and 433 nm and these bands were seen to decrease in the dispersion, presumably as a result of π–π interactions between the MWCNTs and the SPBIBI. Moreover, SPBIBI exhibited a considerable fluorescence emission at 564 nm. After dispersion of the MWCNTs in the polymer solution (MWCNTs/SPBIBI mass ratio is 1/4), 65.6% of the fluorescence emission became quenched. This was probably due to electron transfer and/or energy transfer [54], suggesting a very strong interaction. Furthermore, stacking π–π interactions were presumed to exist between the SPBIBI and the MWCNTs.

3.2. Preparation of MWCNTs/SPBIBI composite membranes

A previous paper has reported on the sulfonated poly [bis(benzimidazobenzisoquinolinones)] (SPBIBI) being thermo-oxidative, hydrolytically and dimensionally stable as a proton exchange membrane [47,48]. However, the proton conductivity for the practical application required further improvement. Novel nanocomposites of MWCNTs and SPBIBI provide new opportunities

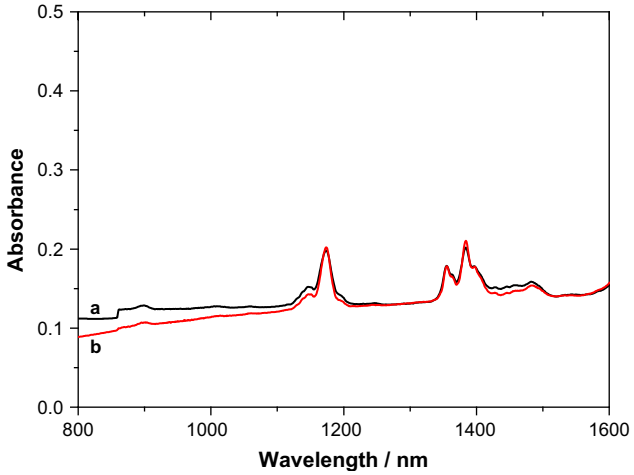

Fig. 3. UV–vis–near IR spectra of a) MWCNTs/SPBIBI (mass ratio: 1:4) dispersion, b) the same dispersion after six months of storage at room temperature.

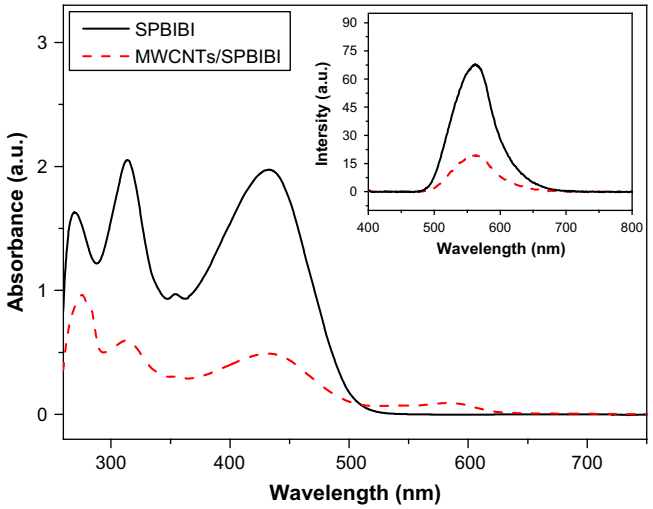

Fig. 5. UV–vis spectra and fluorescence spectra (inset) of pristine SPBIBI and a MWCNTs/SPBIBI (mass ratio: 1: 4) dispersion in DMSO.

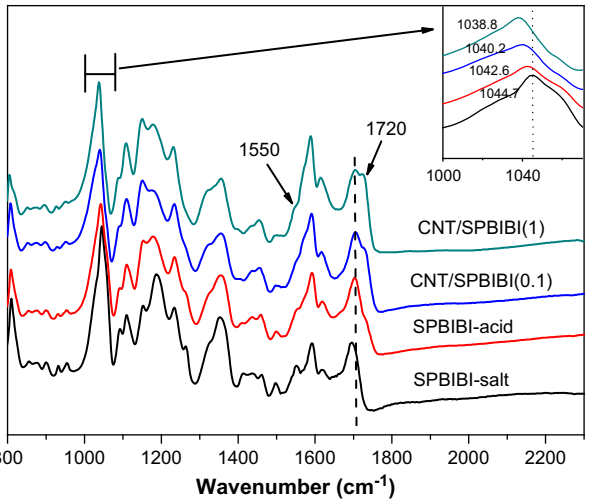

Fig. 6. ATR/FT-IR spectra of the pristine SPBIBI membranes in salt and acid forms as well as of the composite membranes. The inset shows the shift of the $-SO_3^-$ symmetric stretching vibrations.

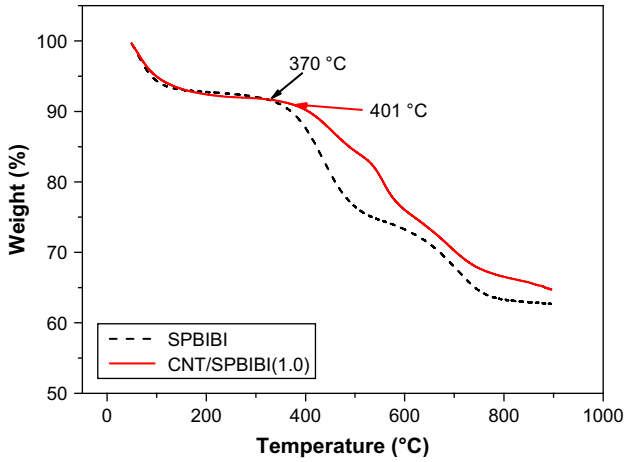

Fig. 7. TGA curves of MWCNTs/SPBIBI(1.0) and pristine SPBIBI membranes under flowing nitrogen.

for improving the performance of SPBIBI materials, especially for proton conductivity. For proton exchange membrane applications, the mass ratio of MWCNTs/SPBIBI dispersions was controlled to less than 5% in order to avoid any short-circuiting in the fuel cells [40]. A simple casting of the dispersions on a glass substrate and successive drying at 100 °C for 12 h and at 150 °C in vacuum for 12 h provided homogeneous composite membranes. A visual examination of the composite membranes revealed a darkening of the membranes as the MWCNTs loading level was increased. No aggregation or void structure was visible.

The membranes were probed with ATR-IR and TGA to examine the interactions between SPBIBI and the MWCNTs and the IR spectra of the composite membrane in the 600–1900 cm^{-1} region are shown in Fig. 6. For the sake of comparison, the acid and salt forms of the pristine SPBIBI were also studied. The characteristic absorption bands at 1702 cm^{-1} were ascribed to the symmetric stretching of the C=O groups, while those at 1617 and 1548 cm^{-1} were assigned to the =C=N stretching vibration. As compared to the pristine SPBIBI in salt form, the C=O absorption bands of the membrane in acid form were shifted up due to the acid–base interaction between the pyridinone ring and sulfonic acid groups, which resulted in a stronger polarization of the C=O bond. In addition, there was a shoulder band around 1720 cm^{-1} for the SPBIBI in acid form and its intensity was seen to increase as the MWCNTs were introduced. It was assumed that the acid–base interaction and the electron and/or energy transfer, increased the polarization of the C=O bond, thus leading to the increased absorption bands at 1720 cm^{-1}. The absorption bands around 1040 cm^{-1} were attributed to the stretching vibration of $-SO_3^-$. A progression in the maximum of the symmetric stretching bands toward a lower wavenumber was observed as the MWCNTs concentration increased from 1038.8 cm^{-1} for the MWCNTs/SPBIBI(1.0) to 1044.7 cm^{-1} for the pristine membrane in salt form (Fig. 6). The result was also attributed to the acid–base interaction and the electron and/or energy transfer which decreased the frequencies of the $-SO_3^-$ stretching peak [55,56].

3.3. The thermal stability and mechanical properties of composite membranes

TGA was employed to characterize the incorporation of MWCNTs into SPBIBI. Fig. 7 shows the TGA curve of the MWCNTs/SPBIBI(1.0) composite membrane as well as that of the membrane of pristine SPBIBI. In the curve corresponding to the composite membrane, three apparent drops in the sample's weight could be observed over the temperature ranges 50–150, 320–450 and 500–750 °C. Similar results were seen in the curve of the pristine SPBIBI membrane. The first weight loss was assigned to the evaporation of hydrated water and the second to the decomposition of the sulfonic acid groups. The on-set decomposition temperature for the second step of the MWCNTs/SPBIBI composite membrane was approximately 30 °C higher than that of its pristine SPBIBI counterpart. The electron and/or energy transfer between the polymer and the MWCNTs could be responsible for the higher desulfonation temperature of the MWCNTs/SPBIBI composite membrane. The last weight loss, which started around 600 °C, was attributed to the decomposition of the polymer backbone. The IR and TGA results also confirmed the existence of a molecular-level interaction between SPBIBI and the MWCNTs.

The mechanical properties of the MWCNTs/SPBIBI composite membranes are summarized in Table 1. The tensile strength and young's modulus of the MWCNT/SPBIBI composite membrane (5.0 wt% MWCNTs) were determined as 126.4 MPa and 1.40 GPa, which are higher than those of the pristine SPBIBI membranes (98.4 MPa of tensile strength, 1.04 GPa of young's modulus). The result indicated that the mechanical properties of the SPBIBI membrane were reinforced with addition of the MWCNTs to the membrane. Similar phenomena were also been reported in polyimide or polybenzimidazole/SWCNTs composites [44,46].

3.4. Morphology analysis

Although the polymer morphology appears to play a dominant role in proton conduction, a systematic relationship between the structure of a polymer and its proton conductivity has yet to be

Table 1
The mechanical properties of MWCNTs/SPBIBI composite membranes.

Sample	Tensile strength (MPa)	Young's modulus (GPa)	Elongation at break (%)
CNT/SPBIBI(0.05)	101.5	1.15	32.9
CNT/SPBIBI(0.1)	110.9	1.18	34.1
CNT/SPBIBI(0.5)	115.8	1.22	36.3
CNT/SPBIBI(1.0)	120.7	1.34	34.5
CNT/SPBIBI(2.0)	124.0	1.39	35.2
CNT/SPBIBI(5.0)	126.4	1.40	34.7
SPBIBI	98.4	1.07	35.8

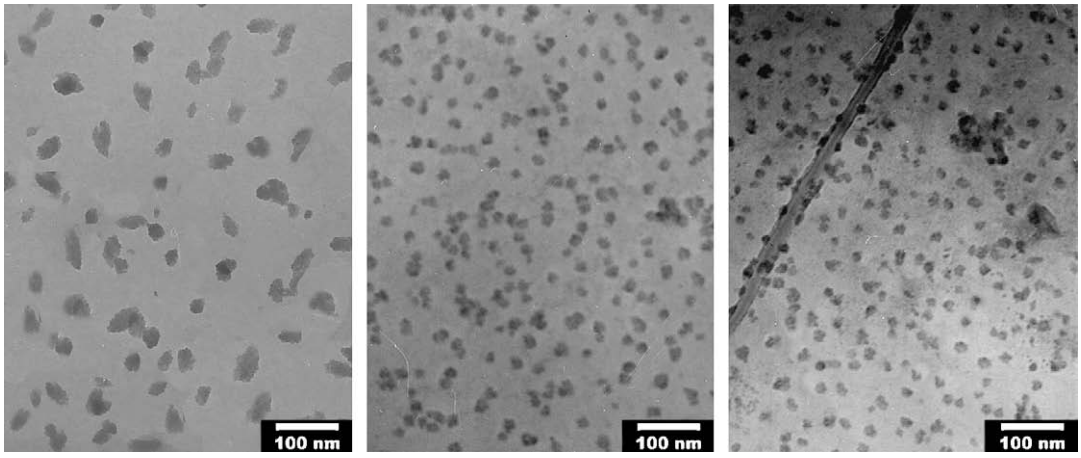

Fig. 8. TEM micrographs of a) pristine SPBIBI, b) MWCNTs/SPBIBI(0.05), and c) MWCNTs/SPBIBI(1.0).

revealed [57–60]. For this reason, the morphological structure of the composite membrane was investigated with transmission electron microscopy (TEM). Thin films were cast from a DMSO solution and stained with lead acetate for the TEM analyses. Fig. 8 shows the morphology of MWCNTs/SPBIBI along with that of pristine SPBIBI. The dark areas represent hydrophilic (ionic) domains whereas the brighter ones refer to hydrophobic regions. Cluster-like ion domains, approx. 60 nm in size, were observed in the pristine SPBIBI membrane. Surprisingly, the addition of merely 0.05 wt% of MWCNTs to the SPBIBI matrix gave rise to changes in the morphological structures. These changes consisted in the ionic clusters in the composite membrane being smaller, approximately 30 nm in size, more uniform and denser than their counterparts in the pristine SPBIBI membranes. It would be interesting to determine how this change in morphology affects water uptake, proton conductivity and methanol transportation.

3.5. Water uptake and dimensional change

The water uptake in a proton-conducting membrane is an important factor that directly influences proton transportation. The water uptake is typically a function of the degree of sulfonation or the ion exchange capacity (IEC); a measure of the exchangeable protons in the material. Furthermore, the morphological structure of the membranes also affects the water uptake. This parameter was determined from the ratio of the weight of the water absorbed by the membrane after immersion and the dry membrane weight. It can also be expressed as the number of H_2O molecules per sulfonic acid group (λ). Table 2 and Fig. 9 compare measured water uptake and λ values of composite membranes of varying MWCNT concentrations with those of Nafion 117 membranes. Each sulfonic acid group of the SPBIBI membranes was solvated by fewer than 8 water molecules, a value much lower than that of Nafion 117 ($\lambda = 12.1$) and other proton-conducting sulfonated aromatic polymers [3]. This lower water uptake was attributed to the combination of a rigid polymer backbone and acid–base interactions between the pyridinone ring and the sulfonic acid groups [47,48]. Nevertheless, the composite membranes possessing similar IEC values displayed a higher water uptakes than the pristine SPBIBI membrane. The composite membrane MWCNTs/SPBIBI(0.5), for example, showed a water uptake of 40.1% and λ value of 7.8. This was higher than the corresponding results for the SPBIBI membrane (32.9% water uptake, $\lambda = 5.4$). Based on the results of the microscopic observation, the morphology of the composite membranes—consisting in smaller ionic clusters—was believed to be responsible for the higher water uptake in the composite as opposed to in their pristine counterparts. This was presumably due to the formation of small ionic clusters allowing for a more continuous and cohesive hydrophilic matrix providing a greater number of hydrophilic sites for water uptake. However, as the content of MWCNTs was further increased, a decreased in water uptake was obtained. The composite membrane MWCNTs/SPBIBI(5.0) with the high content of MWCNTs showed a lower water uptake than its counterparts, and this was ascribed to the IEC decreased and/or that the high content of hydrophobic MWCNTs occupied the volume available for water absorption.

Table 2
Water uptake and swelling ratio of SPBIBI composite membranes.

Sample	IEC (mequiv g^{-1})	Water uptake (wt%)		Swelling ratio (%)	
		20 °C	λ	Δl	Δt
CNT/SPBIBI(0.05)	2.87	37.8	7.3	3.9	13.9
CNT/SPBIBI(0.1)	2.87	38.2	7.4	4.1	13.8
CNT/SPBIBI(0.5)	2.86	40.1	7.8	4.2	14.9
CNT/SPBIBI(1.0)	2.84	39.1	7.6	4.2	14.2
CNT/SPBIBI(2.0)	2.81	37.2	7.4	3.8	13.2
CNT/SPBIBI(5.0)	2.73	28.1	5.7	3.2	10.0
SPBIBI	2.87	32.9	6.4	4.0	11.2
Nafion 117	0.9	19.4	12.0	11.4	13.2

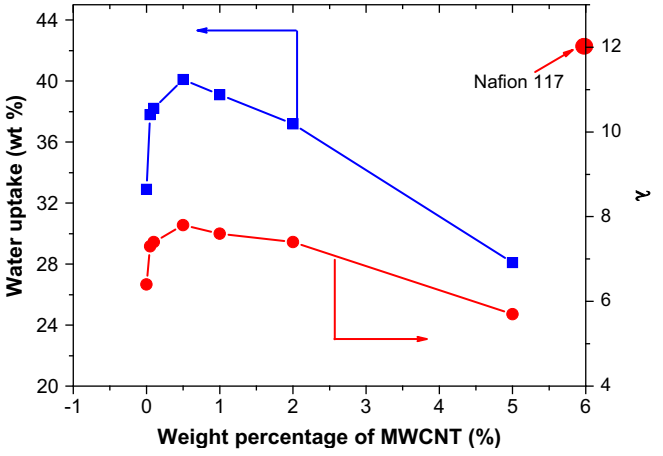

Fig. 9. A plot of the water uptake and lamda vs weight percentage of MWCNTs for MWCNTs/SPBIBI composite membranes.

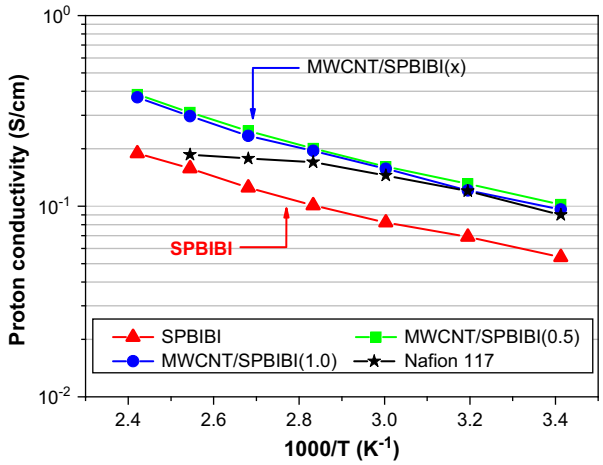

Fig. 10. The temperature dependence of proton conductivity for membranes of SPBIBI, two composites and Nafion 117 membranes between 20 and 140 °C.

The membranes' dimensional change along the in-plane and through-plane directions of the sample due to water sorption at under fully hydrated conditions is presented in Table 2. The dimensional change was found to strongly depend on the water uptake, and the general trend was that a higher water uptake led to membranes with a more considerable dimensional change. Although all the composite membranes showed similar in-plane swelling, a higher swelling ratio in through-plane directions of composite membrane was observed due to the higher water uptake. Furthermore, these membranes show unisotropic dimensional changes between in-plane and through-plane directions. For example, the MWCNTs/SPBIBI(0.5) membrane showed more than 3 times larger swelling in through-plane direction (14.1%) than in-plane direction (4.2%). The higher water uptake and through-plane swelling may also suggest the formation of ordered hydrophilic domains within the composite membranes.

3.6. Electron and proton conductivities

As discussed above, in order to avoid any short-circuiting in the fuel cell, the membrane should not be electrically conductive, and thus, the carbon nanotubes should not percolate. The electron conductivity of the membranes was measured and the data is tabulated in Table 3. The Nafion 117 displayed an electrical conductivity of 2.1×10^{-6} S cm^{-1}, which agreed well with results presented in the literature [61]. The electron conductivity of the pristine SPBIBI membrane was 3.4×10^{-6} S cm^{-1}, and this value was slightly higher than that of Nafion 117. The electron conductivity of the composite membranes increased as the MWCNTs content was raised. In comparison to the pristine SPBIBI, these results were high but still lower than 10^{-4} S cm^{-1}. With such values, there would be no risk of a short circuit occurring during the fuel cell test operation [40]. Furthermore, the result indicated that the mere presence of MWCNTs was inadequate for forming an electronically conducting network. The interaction between the MWCNTs and the SPBIBI effectively blocked the conduction of electrons, and it was assumed that the high affinity of the polymer to the MWCNT surfaces allowed the polymers to completely coat and insulate these surfaces. The MWCNTs and MWCNT bundles were thus coated with the insulative polymer in such a way as to prevent the charge from transferring from one MWCNT bundle to another.

Table 3
The electron and proton conductivity of SPBIBI composite membranes.

Sample	Electron conductivity (10^{-6} S cm^{-1})	Proton conductivity (10^{-3} S cm^{-1})	
		σ^a	σ^b
CNT/SPBIBI(0.05)	3.9	78.0	16.4
CNT/SPBIBI(0.1)	5.1	89.0	17.0
CNT/SPBIBI(0.5)	6.9	102.0	21.0
CNT/SPBIBI(1.0)	7.2	94.0	18.0
CNT/SPBIBI(2.0)	9.8	90.0	18.0
CNT/SPBIBI(5.0)	89.0	71.0	15.8
SPBIBI	3.4	54.0	5.1
Nafion 117	2.9	90.0	20.0

[a] Measured in water at 20 °C.
[b] Measured at 70 °C, 50% relative humidity.

In PEM fuel cells, the proton conductivity of the membrane is particularly important since it plays a significant role in fuel cell performance. To achieve good conductivity, an extensively phase-separated morphology or high acid loading (water uptake) is desirable. Table 3 showed the proton conductivity of the membranes under fully and partially hydrated conditions. The composite membranes with similar IEC values displayed significantly higher proton conductivities than their pristine counterpart, especially under partially hydrated condition. More specifically, the composite membranes possessing a MWCNTs content of 0.5 wt% exhibited proton conductivities of 0.021 S cm^{-1} at 70 °C, 50 RH%, which is almost four times higher than that of pristine SPBIBI membrane at the same testing conditions (0.005 S cm^{-1}). This value was comparable to Nafion 117 (0.020 S cm^{-1}). Under fully hydrated condition (in water), such superior values were maintained when the temperature was raised to 140 °C, as shown in Fig. 10. The highest conductivity (i.e., 0.424 S cm^{-1}) was observed for the MWCNTs/SPBIBI(0.5) membrane at 140 °C, and corresponds to more than twice the value of the pristine SPBIBI membrane (0.184 S cm^{-1}, at 140 °C). However, the measurement could not be performed on Nafion 117 at such a high temperature due to a loss of mechanical strength.

Also the composite membrane MWCNTs/SPBIBI(5.0) with an elevated MWCNT content demonstrated a higher proton conductivity than that of the pristine SPBIBI membrane, despite its inferior water uptake. It was found that the composite membranes containing 0.5 wt% MWCNTs showed the best properties in terms of stability and proton conductivity. Although the use of certain MWCNT composites as proton exchange membranes has already been reported, only a limited amount of papers describe the achievement of greatly enhanced proton conductivities. A representative example for the conductive enhancement of a polymer by the addition of sulfonated SWCNTs is the S-SWCNTs/Nafion composite, reported by Kannan et al., [62] in which the addition of 0.05 wt% sulfonated SWCNTs gave rise to an increase in the proton conductivity due to the high sulfonic acid content of the composite membrane. In the present case, our success was attributed to an enhancement of the proton conductivities to the effective load transfer to the MWCNTs as a result of the interaction between the polymer and the MWCNTs, as discussed above. The interaction between the hydrophobic MWCNTs and the polymer main chain increased the hydrophilic/hydrophobic separation of the SPBIBI membranes giving rise to smaller, highly dense and ordered ionic clusters that were able to form enhanced connections for the proton transport pathway. Thus, an improved proton conductivity was observed for the composite membranes.

To further confirm the effect of the MWCNTs on the proton conductivity of SPBIBI membranes, SPBIBI-b based on 1,4,5,8-naphthalenetetracarboxylic dianhydride and sulfonated tetraamine (IEC = 2.56 mequiv g^{-1}) (Fig. 11) was adopted as the matrix [48]. Just as for SPBIBI, the SPBIBI-b composite membrane loaded with

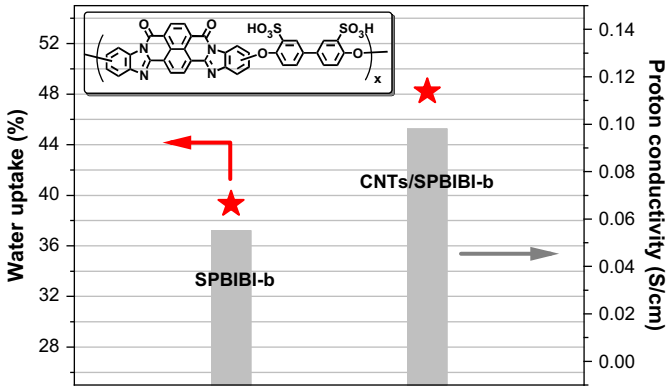

Fig. 11. A comparison of the water uptake and proton conductivity of SPBIBI-b and CNTs/SPBIBI-b(1/100) composite membranes.

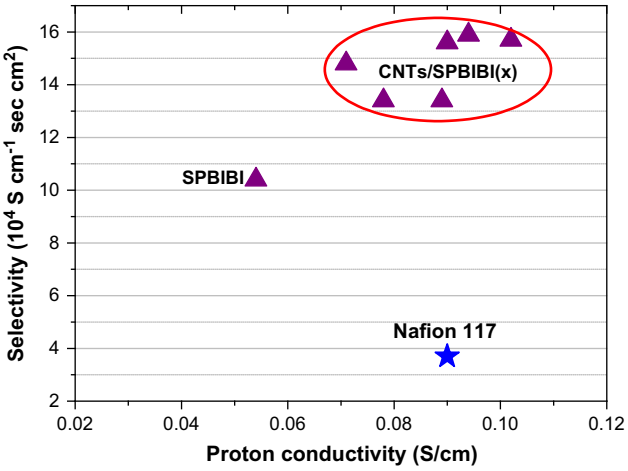

Fig. 12. The performance tradeoff plot of the conductivity vs the selectivity.

1.0 wt% MWCNTs showed a higher water uptake than that of its pristine SPBIBI-b counterpart. As shown in Fig. 11, the proton conductivity of the composite membrane was, at room temperature, almost twofold that of the pristine SPBIBI-b. From these results, it was clear that the homogeneous dispersion of MWCNTs evoked a significant change in morphology along with an improvement in the proton-conducting behavior of the proton exchange membranes.

3.7. Methanol permeability and oxidative stability

Table 4 lists the methanol permeability of the obtained membranes at room temperature (25 °C). The composite membranes showed lower values than that containing Nafion 117 (2.4×10^{-6} cm^2 s^{-1}). However, these results were slightly high as compared to that of the pristine SPBIBI. For example, the MWCNTs/SPBIBI(0.5) composite membrane exhibited a methanol permeability of 6.5×10^{-7} cm^2 s^{-1} as opposed to 5.2×10^{-7} cm^2 s^{-1} for its pristine SPBIBI counterpart. For a fully hydrated membrane, the methanol transport across a proton exchange membrane should be strongly dependent upon the water uptake, due to the methanol permeating through the membranes as complex forms such as $CH_3OH_2^+$ and H_3O^+. The composite membranes presented higher water uptake values, and thus higher methanol permeabilities as compared to the pristine SPBIBI membrane.

In order to understand the performance tradeoff between the permeability and conductivity, an investigation was carried out using the selectivity as a representation of the transport characteristics of both the proton and methanol (σ/P) of the MWCNTs/SPBIBI, SPBIBI and Nafion 117 membranes. The results are shown in Fig. 12. The composite membrane was more selective than its pristine SPBIBI counterpart and approx 5 times more selective than that of Nafion 117. Interestingly, a homogeneous dispersion of the MWCNTs in the SPBIBI membrane increased both the resultant proton conductivity and selectivity. This result differed greatly from those of other composite membranes with hygroscopic inorganic "fillers" in which the selectivity could be increased while sacrificing the proton conductivity [31]. The results indicated that the addition of the MWCNTs into the SPBIBI matrix favored the proton transport but blocked the permeability of methanol.

The oxidative stability of the composite membranes was tested in Fenton's reagent (30 ppm $FeSO_4$ in 30% H_2O_2) at 25 °C and the results can be seen in Table 4. It was fount that the oxidative stability of the membranes decreased with increasing MWCNTs loading levels. The time after which the MWCNTs/SPBIBI composite membranes with 0.05–5 wt% MWCNT content started to break into pieces decreased from 20 h to 15 h. The oxidative stability was thus comparable to that of the pristine SPBIBI membranes that required 18 h to break into pieces.

Table 4
The oxidative stability and methanol permeability of SPBIBI composite membranes.

Sample	Oxidative stability[a]		Methanol permeability (cm^2 s^{-1})
	τ_1[b] (h)	τ_2[c] (h)	
CNT/SPBIBI(0.05)	20	22	5.8×10^{-7}
CNT/SPBIBI(0.1)	20	23	6.4×10^{-7}
CNT/SPBIBI(0.5)	19	22	6.5×10^{-7}
CNT/SPBIBI(1.0)	19	23	5.9×10^{-7}
CNT/SPBIBI(2.0)	16	21	5.9×10^{-7}
CNT/SPBIBI(5.0)	15	21	4.8×10^{-7}
SPBIBI	18	22	5.2×10^{-7}
Nafion 117	–	–	2.4×10^{-6}

[a] 30 °C in 30% H_2O_2 containing 30 ppm $FeSO_4$.
[b] The time when the membrane broke into pieces after being shaken drastically.
[c] The time when the membrane dissolved completely.

4. Conclusions

Sulfonated poly[bis(benzimidazobenzisoquinolinone)] was found to act as a good dispersant for MWCNTs. The MWCNTs/SPBIBI dispersions with the highest MWCNTs concentration of 1.5–2.0 mg mL^{-1} (using a SPBIBI to MWCNTs mass ratio of 4:1) were stable for more than six months at room temperature. MWCNTs/SPBIBI composite membranes could be successfully fabricated and used as proton exchange membranes for fuel cells without any visible aggregation of the MWCNTs. The resultant composite membranes showed much higher proton conductivity values than their pristine SPBIBI counterpart, however without sacrificing other excellent properties (such as dimensional and thermo-oxidative stabilities). The enhanced proton conductivity was attributed to the ordered and smaller cluster-like ion domains of the composite membranes, observed by transmission electron microscopy. Moreover, a high selectivity (σ/P) was observed for the composite membranes as a result of the high proton conductivity. The homogenous dispersion of the MWCNTs, as well as the efficient enhancement performance of the SPBIBI, was due to the interaction between the pyridinone ring and the sidewalls of the MWCNTs which changed the morphological structure of composite membranes as revealed by TEM. Further addition of the MWCNTs to the other aromatic ionomers (such as sulfonated polyimide with conjugated groups in polymer main chain) is expected to enhance

the proton conductivity of composite membranes for fuel cell applications. More detailed investigations are currently in progress in our laboratory.

Acknowledgments

We thank the National Basic Research Program of China (No. 2009CB623401) and the National Science Fund for Distinguished Young Scholars (No. 50825302) for the financial support.

References

[1] Jacobson MZ, Colella WG, Golden DM. Science 2005;308:1901.
[2] Steele BCH, Heinzel A. Nature 2001;414:345.
[3] Hickner MA, Ghassem H, Kim YS, Einsla BR, McGrath JE. Chem Rev 2004;104:4587.
[4] Kreuer KD. J Membr Sci 2001;185:29.
[5] Kreuer KD, Paddison SJ, Spohr E, Schuster M. Chem Rev 2004;184:4637.
[6] Gamburzev S, Appleby AJ. J Power Sources 2002;107:5.
[7] Takimoto N, Wu L, Ohira A, Takeoka Y, Rikukawa M. Polymer 2009;50:534.
[8] Shoesmith JP, Collins RD, Oakley MJ, Stevenson DK. J Power Sources 1994;49:129.
[9] Lemons R. J Power Sources 1990;29:251.
[10] Scott K, Taama WM, Argyropoulos P, Sundmacher K. J Power Sources 1999;83:204.
[11] Jagur-Grodzinski J. Polym Adv Technol 2007;18:785.
[12] Harrison WL, Wang F, Mecham JB, Bhanu V, Hill M, Kim YS, et al. J Polym Sci Part A Polym Chem 2003;41:2264.
[13] Wang F, Hickner M, Kim YS, Zawodzinski TA, McGrath JE. J Membr Sci 2002;197:231.
[14] Ueda M, Toyota H, Ochi T, Sugiyama J, Yonetake K, Masuko T, et al. J Polym Sci Part A Polym Chem 1993;31:853.
[15] Genies C, Mercier M, Sillion B, Cornet N, Gebel G, Pineri M. Polymer 2001;42:359.
[16] Miyatake K, Higuchi E, Watanabe M. J Am Chem Soc 2007;129:3879.
[17] Li N, Cui Z, Zhang S, Xing W. Polymer 2007;48:7255.
[18] Zhang F, Cui Z, Li N, Dai L, Zhang S. Polymer 2008;49:3272.
[19] Roy A, Lee H, McGrath JE. Polymer 2008;23:5037.
[20] Savard O, Peckham TJ, Yang Y, Holdcroft S. Polymer 2008;49:4949.
[21] Kumbharkar SC, Islam M, Potrekar RA, Kharul UK. Polymer 2009;50:1403.
[22] Schberger F, Chromik F, Kerres J. Polymer 2009;50:1403.
[23] Bai Z, Houtz MD, Mirau PA, Dang TD. Polymer 2007;48:6598.
[24] Zhao C, Wang Z, Bi D, Lin H, Shao K, Fu T, et al. Polymer 2007;48:3090.
[25] Borup R, Meyers J, Pivovar B, Kim YS, Mukundan R, Garland N, et al. Chem Rev 2007;107:904.
[26] Xie T, Hayden CA. Polymer 2007;48:5497.
[27] Ladewig BP, Knott RB, Hill AJ, Riches JD, White JW, Martin DJ, et al. Chem Mater 2007;19:2372.
[28] Rhee CH, Kim HK, Chang H, Lee JS. Chem Mater 2005;17:1691.
[29] Truffier-Bountry D, De Geyer A, Guetaz L, Diat O, Gebel G. Macromolecules 2007;40:8259.
[30] Chen WF, Kuo PL. Macromolecules 2007;40:1987.
[31] Jiang SP, Liu Z, Tian ZQ. Adv Mater 2006;18:1068.
[32] Deng WQ, Molinero V, Goddard WA. J Am Chem Soc 2004;126:15644.
[33] Reneker DH, Yarin AL. Polymer 2008;49:2387.
[34] Andrews R, Jacques D, Qian D, Rantell T. Acc Chem Res 2002;35:1008.
[35] Sun YP, Fu K, Lin Y, Huang W. Acc Chem Res 2002;35:1096.
[36] Ajayan PM. Chem Rev 1999;99:1787.
[37] Landi BJ, Raffaelle RP, Heben MJ, Alleman JL, VanDerveer W, Gennett T. Nano Lett 2002;2:1329.
[38] Wang J, Musameh M, Lin Y. J Am Chem Soc 2003;125:2408.
[39] Liu YH, Yi B, Shao ZG, Wang L, Xing D, Zhang H. J Power Sources 2007;163:807.
[40] Thomassin JM, Kollar J, Caldarella G, Germain A, Jerome R, Detrembleur C. J Membr Sci 2007;303:252.
[41] Kim JY, Han S, Hong S. Polymer 2008;49:3335.
[42] Laskoski M, Keller TM, Qadri SB. Polymer 2007;48:7484.
[43] Chen H, Liu Z, Cebe P. Polymer 2009;50:872.
[44] Delozier DM, Watson KA, Smith JG, Clancy TC, Connell JW. Macromolecules 2006;39:1731.
[45] Licea-Jimenez L, Grishina AD, Pereshivko LY, Krivenko TV, Savelyev VV, Rychwalski RW, et al. Carbon 2005;44:113.
[46] Okamoto M, Fujigaya T, Nakashima N. Adv Funct Mater 2008;18:1.
[47] Li N, Zhang S, Liu J, Zhang F. Macromolecules 2008;41:4165.
[48] Li N, Cui Z, Zhang S, Xing W. J Membr Sci 2009;326:420.
[49] Zou J, Liu L, Chen H, Khondaker SI, McCullough RD, Huo Q, et al. Adv Mater 2008;20:2055.
[50] Gu H, Swager TM. Adv Mater 2008;20:1.
[51] O'Connell MJ, Bachilo SM, Huffman CB, Moore VC, Strano MS, Haroz EH, et al. Science 2002;297:593.
[52] Star A, Stoddart JF, Steuerman D, Diehl M, Boukai A, Wong EW, et al. Angew Chem Int Ed 2001;40:1721.
[53] Chen J, Liu H, Weimer WA, Halls MD, Waldeck DH, Walker GC. J Am Chem Soc 2002;124:9034.
[54] Fan C, Wang S, Hong JW, Bazan GC, Plaxco KW, Heeger AJ. Proc Natl Acad Sci USA 2003;100:6297.
[55] Park HS, Kim YJ, Hong WH, Choi YS, Lee HK. Macromolecules 2005;38:2289.
[56] Tannenbaum R, Rajagopalan M, Eisenberg A. J Polym Sci Part B Polym Phys 2003;41:1814.
[57] Eisenberg A, King M. Ion conducting polymers: physical properties and structures. New York: Academic Press; 1977.
[58] Ding JF, Chuy C, Holdcroft S. Chem Mater 2001;13:2231.
[59] Maki-Ontto R, de Moel K, Polushkin E, van Ekenstein GA, ten Brinke G, Ikkala O. Adv Mater 2002;14:357.
[60] Yoshio M, Kagata T, Hoshino K, Mukai T, Ohno H, Kato T. J Am Chem Soc 2006;128:5570.
[61] Chen WF, Wu JS, Kuo PL. Chem Mater 2008;20:5756.
[62] Kannan R, Kakade BA, Pillai VK. Angew Chem Int Ed 2008;47:2653.